JOURNAL OF MATERIALS SCIENCE 22 (1987) 907–914

Initiation and early growth mechanisms of corrosion fatigue cracks in stainless steels

R. MATHIS
Max-Planck-Institut für Plasmaphysik, 8046 Garching, FRG

The mechanism of corrosion fatigue crack initiation in stainless steels was examined in both air and chloride solutions. For a tempered martensitic, a duplex and a soft martensitic steel it is shown that the decrease of the fatigue strength from the value measured in air to that measured in corrosive environments depends primarily upon the stability of the protective film. If the passivity is stable, cracks are found to originate almost exclusively at oxide inclusions. Cracking or debonding were found to occur. For the duplex steel in the vicinity of the inclusion there were pronounced emerging persistent slip bands. They cause localized corrosion attack, thus allowing cracks to be formed more easily. If pitting is superposed, crack nucleation always occurs at the base of the pit. Pit formation and growth rate are accelerated by cyclic loading.

1. Introduction

The mechanism of corrosion fatigue crack initiation is most important for the cyclic lifetime of structural members made from stainless steels. A crack once initiated cannot be prevented from propagating and the cyclic lifetime is dominated by the formation time of cracks. Fatigue crack initiation in technical materials normally starts at the surface. Surface crystals are more easily deformed, interaction with the surroundings is possible, and notches already present or due to plastic deformation newly formed act as stress raisers. During cyclic deformation, shear stresses initiate the motion of dislocations. If the same glide plane is frequently activated, at surface crystals these dislocations lead to the well-known concentration of slip to a few "persistent slip bands" (PSBs) [1]. The plastic deformation occurring in cyclically stressed technical materials below the fatigue limit as well is localized to these areas. The formation of intrusions and extrusions is closely related to this phenomenon. The correlation between crack nucleation and PSBs is due first of all to localized stress regions resulting from the surface topography. It was found that PSBs themselves contain microembryonic cracks. These are created either by vacancy generation within the plastically deformed region [2] or by decohesion at the matrix–slip band interface [3]. There, crack formation is facilitated by the release of stored elastic energy (inner stresses). Another conceivable crack formation model also starts with coarse slips, and so the crack nucleation arises from the necessity of activating two or more slip systems, each perpendicular to the previous one (valid for symmetric push–pull loading) [4].

In polycrystals and complex alloys inhomogeneities such as grain and phase boundaries or segregations but especially inclusions, play an important role in influencing fatigue failure [5–7]. Owing to their different elastic properties, inclusions in matrix materials serve as stress raisers. In real high-cycle fatigue, microplasticities (PSBs) may lead to debonding of the inclusion–matrix interface or cracking of the inclusion itself. Fatigue cracks in steels are predominantly nucleated at inclusions located at surfaces [5, 6, 8].

Stainless steels in aqueous solutions may be protected from corrosion by a passive film. In the stable passive state, the corrosion rate is zero to a first approximation. Under certain conditions reaction processes cause local breakdown of protective films (unstably passive) [9]. Apart from active pit areas caused by, for example, chloride ions, the steel surface here is passive. Such localized attacks on stainless-steel surfaces – further possibilities are intergranular corrosion and preferential attack on inclusions or the surrounding matrix owing to their different corrosion potentials – can often be directly associated with the initiation of corrosion fatigue cracks.

Corrosion fatigue crack initiation can be most simply described as normal fatigue crack initiation interacting with corrosive environmental effects. Different theories are conceivable to explain the facilitating of crack nucleation by environmental effects [1, 9–14]: localized corrosion such as pitting, preferential dissolution of deformed areas such as PSBs which are anodic to the matrix, localized rupture of passive film by emerging PSBs causing the exposure of unprotected metal, and reduction of surface energy by adsorption of anions from the environment.

The purpose of this paper is to show the initiation mechanism and the early growth of corrosion fatigue cracks in stainless steels in conjunction with corrosion pitting, non-metallic inclusions and PSBs.

2. Materials and experimental procedures

The following types of steel were used in the investigations: a tempered martensitic 13 wt % Cr, a ferritic–

0022–2461/87 $03.00 + .12 © *1987 Chapman and Hall Ltd.*

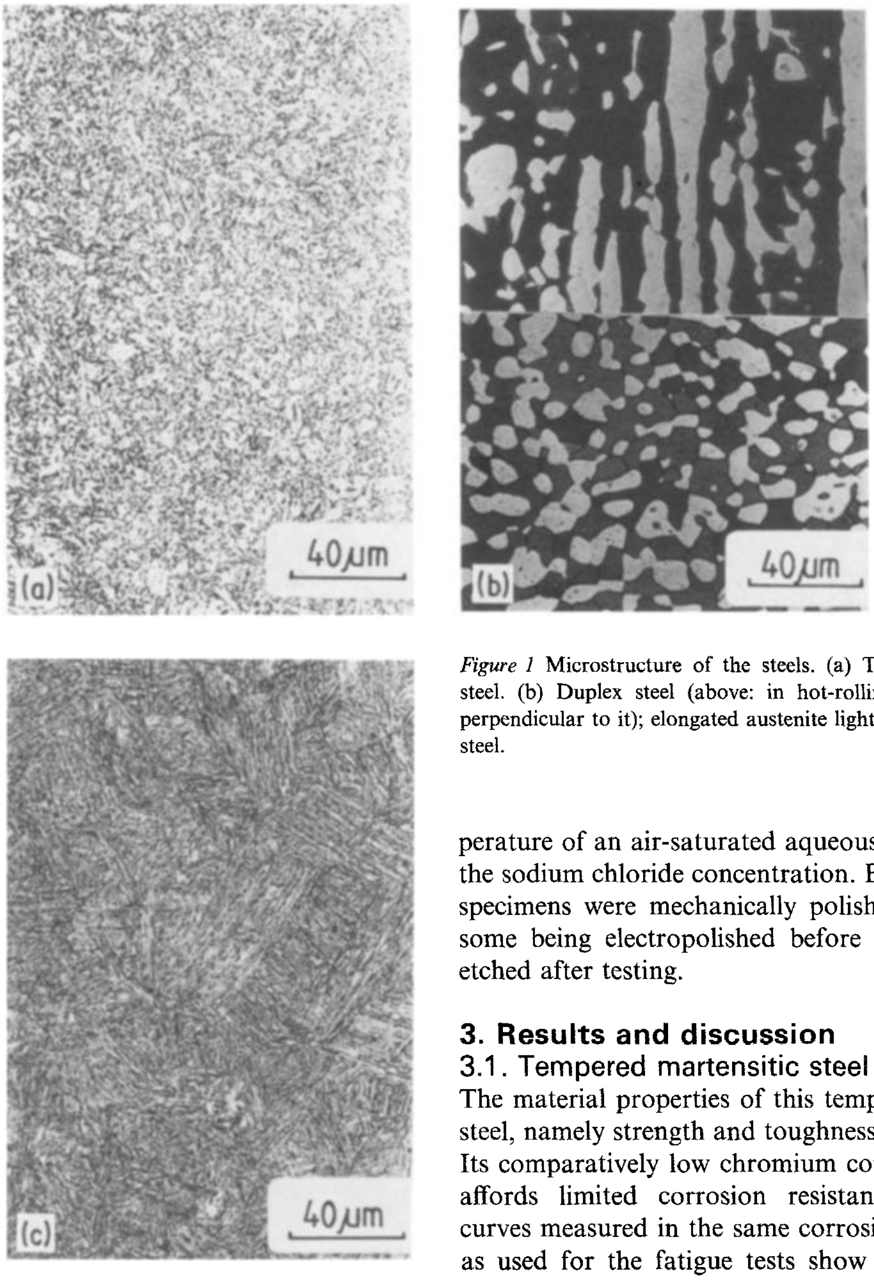

Figure 1 Microstructure of the steels. (a) Tempered martensitic steel. (b) Duplex steel (above: in hot-rolling direction; below: perpendicular to it); elongated austenite light. (c) Soft martensitic steel.

austenitic 22 % Cr–5 % Ni duplex, and a soft martensitic 16 % Cr–5% Ni steel [15, 16]. The alloy compositions and mechanical properties of these steels are listed in Table I; the microstructures are shown in Fig. 1.

The corrosion fatigue tests with a sinusoidal load wave (frequency 50 Hz) were performed at stress ratios $R = \sigma_{\max}/\sigma_{\min} \geqslant 0$ in a uniaxial tension stress field. They consisted in determining the corrosion fatigue limit and the crack mechanism under conditions of free corrosion as a function of the temperature of an air-saturated aqueous solution and of the sodium chloride concentration. Before testing, all specimens were mechanically polished and cleaned, some being electropolished before and some being etched after testing.

3. Results and discussion

3.1. Tempered martensitic steel

The material properties of this tempered martensitic steel, namely strength and toughness, are quite good. Its comparatively low chromium content of 13 wt % affords limited corrosion resistance. Polarization curves measured in the same corrosive environments as used for the fatigue tests show that under conditions of free corrosion the steel surface is exposed to an electrochemical potential at which pitting will be initiated and propagated [16].

As the solution temperature increases, the real high-cycle corrosion fatigue strength ($\geqslant 10^7$ cycles) permanently decreases from the air fatigue limit of 330 MN m^{-2} to less than 50 MN m^{-2} at 150° C. The S–N curves obtained for this steel clearly show the absence of a corrosion fatigue limit even for fatigue lifetimes for which a limit still exists in air (Fig. 2).

The high-cycle fatigue crack initiation in air is associated exclusively with surface inclusions, whereas

TABLE I Nominal and actual compositions, heat treatments and mechanical properties of the steels

Steel	Chemical composition (wt %)					Heat treatment	Mechanical properties at 20° C (MN m^{-2})	
	C	Cr	Ni	Mo	N		0.2% proof strength	Tensile strength
Tempered martensitic (X20Cr13)	0.14	12.5	–	–	–	1000° C, 30 min; 700° C, 60 min	620	790
Ferritic–austenitic (X2CrNiMoN22 5)	0.02	20.7	5.4	3.2	0.19	1050° C, 60 min	470	700
Soft martensitic (X4CrNiMo16 5)	0.03	15.1	5.1	0.9	–	1000° C, 60 min; 2 × 580° C, 240 min	765	930

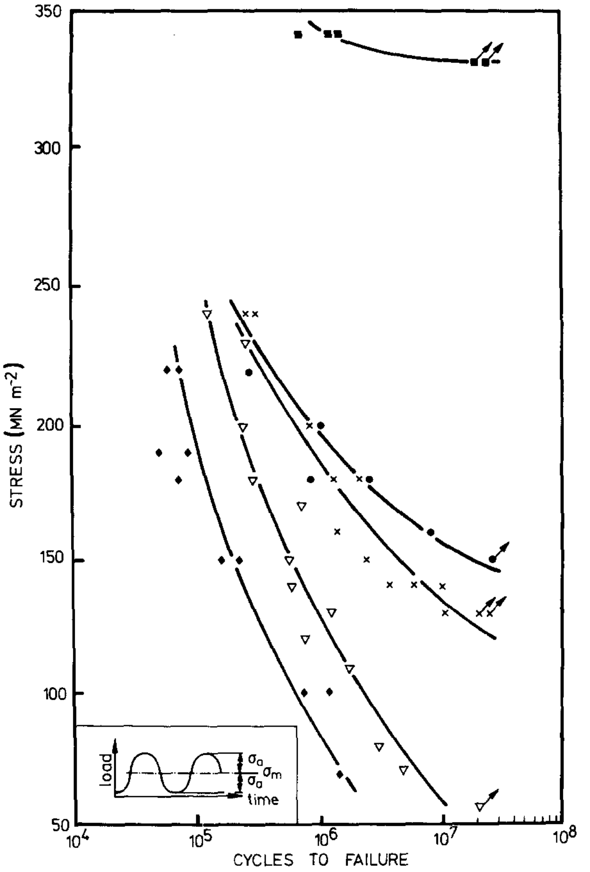

Figure 2 Tempered martensitic steel: air and corrosion fatigue behaviour. (■) Air; (●) 20° C, 0.01 N NaCl; (x) 80° C, 0.01 N NaCl, (▽) 80° C, 4.4 N NaCl; (◆) 150° C, 0.01 N NaCl. σ_m = 250 MN m^{-2}, 50 Hz.

cracks propagating in corrosive environments were only found to originate from corrosion pits (Fig. 3). Nevertheless, initiation of pitting at stainless-steel surfaces in chloride environments mostly starts at non-metallic inclusions [17]. This nucleation and propagation may be accelerated by applying dynamic loads.

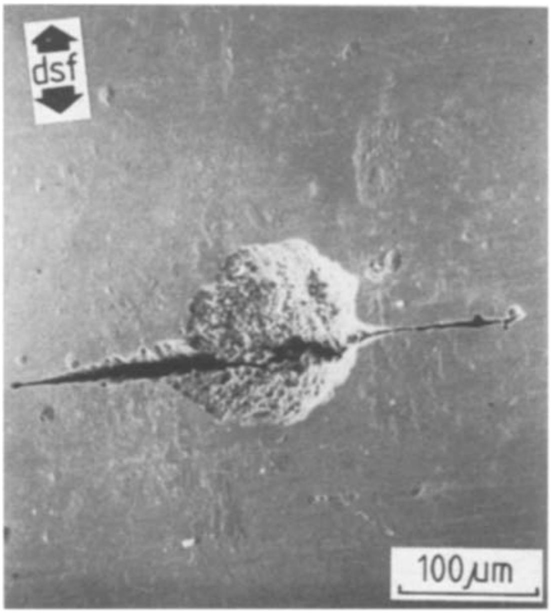

Figure 3 Tempered martensitic steel: crack initiation at the base of a corrosion pit (dsf = direction of uniaxial stress field); surface photograph.

Local yielding of metal will lead to enhanced dissolution. The main effect of pitting on corrosion fatigue crack initiation, apart from intensifying the stress at the base of the pit, is that it changes the electrochemical conditions within the pit [18]. The non-existence of a corrosion fatigue limit is related to the time-dependent crack growth of the pits and thus to the normally increasing stress concentration effect at the base of the pit. In most specimens few, but usually more than one, crack nuclei could be detected.

Hydrogen-assisted crack initiation is another possible failure mechanism [19]. As a result of the anodic dissolution within the pit, hydrogen may be produced and lead to a brittle fracture process due to hydrogen absorption. The stress field around the pit may lead to diffusion of hydrogen into the zone ahead of the pit, and a crack nucleus may be formed by hydrogen embrittlement. The failure of the fractographic features produced by this mechanism in such steels (presence of grain boundary or quasi-cleavage facets, often showing brittle striations) excludes the presence of hydrogen-induced (fatigue) crack initiation under these conditions.

The crack initiation mechanism for this tempered martensitic steel in NaCl solutions is found to be due to the superposition of pitting and corrosion fatigue. The dynamic loads applied may decrease the induction time for pit nucleation and increase the pit growth rate. The transition from (accelerated) pit growth to corrosion fatigue crack nucleation is not well defined; the initiation process itself may occur at PSBs at the base or equator of the pit.

3.2. Ferritic–austenitic steel

Such duplex steels combine the good resistance of ferritic steels to chloride-induced stress corrosion cracking and the high resistance of austenitic steels to hydrogen-induced stress corrosion cracking. Measurement of the corrosion rate against potential curves in a "corrosion fatigue test environment" has shown a higher resistance to pitting in NaCl solutions than would be expected from the alloy composition. Pitting should thus not occur under conditions of free corrosion in these solutions up to temperatures of 100° C [15, 20].

The duplex steel clearly shows the effect of corrosion behaviour on corrosion fatigue. Up to temperatures of 80° C, even in concentrated chloride solutions, the fatigue strength at high cycles only decreases from the air value of 240 MN m^{-2} to 200 MN m^{-2} (Fig. 4). Under these stably passive corrosion conditions stainless steel also shows a fatigue limit. On specimen surfaces or fractures no corrosion attack can be macroscopically detected. Microscopically, however, a localized corrosion attack caused by emerging PSBs on austenitic grain surfaces is visible (Fig. 5).

At high stress levels corrosion fatigue crack initiation occurs mainly at PSBs in austenite or near phase boundaries (Fig. 6), whereas non-metallic surface inclusions affect the initiation mechanism at lower stress levels (Fig. 7). PSBs are due to the intensified stress field caused by the different elastic properties of

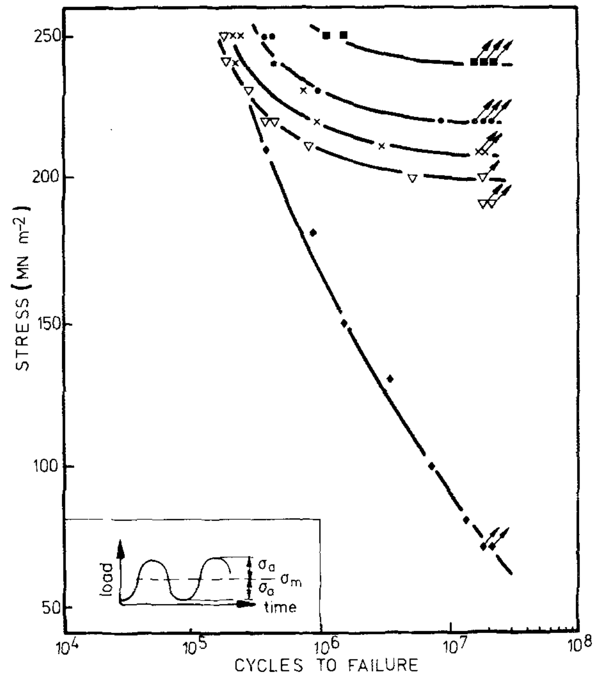

Figure 4 Duplex steel: air and corrosion fatigue behaviour. (■) Air; (●) 20° C, 0.01 N NaCl; (x) 80° C, 0.01 N NaCl, (▽) 80° C, 4.4 N NaCl; (◆) 150° C, 0.01 N NaCl. $\sigma_m = 250\,\text{MN}\,\text{m}^{-2}$, 50 Hz.

the inclusion and matrix, and are thus concentrated around the particles (Fig. 7). In the high-cycle range of corrosion fatigue the bulk cyclic strain remains within the elastic range and all cyclic–plastic strains are confined to small regions surrounding the inclusion. The adhesion between the matrix and oxide inclusion is mostly sufficiently high, with no debonding of the interface normally occurring. The bonding does not seem to be significantly affected by corrosion reactions either. Only in isolated cases has debonding of the interface also been observed (Fig. 8). Stringers of manganese sulphide, which are ineffectual stress raisers but are preferred points of localized corrosion attack, were not found to initiate corrosion fatigue cracks. The fractographic features of crack nucleations in air, apart from corrosion products, are the same as observed in corrosive environments if the protective film remains stable.

At elevated solution temperatures these ferritic–austenitic stainless steels exhibit no stable passivity. Here pitting corrosion is superposed, and the corrosion fatigue strength is significantly decreased. The crack nucleation mechanism is similar to that described for the 13 % Cr steels. If the duplex steel is protected from localized corrosion by a stable film, only one or very few corrosion fatigue crack nucleations can be detected, whereas there is usually more than one propagating crack visible if pitting is superposed. No indications of hydrogen-assisted crack initiation were found. Investigations carried out by Moskovitz and Pelloux [21] for some duplex steels show similar results.

The following mechanisms of corrosion fatigue crack nucleation for this duplex steel in NaCl solutions up to temperatures of 80° C (stable passive corrosion conditions) are conceivable:

1. At high load levels initiation will occur in the bulk (caused by, for example, emerging PSBs) as well as at inclusions.
2. At lower stress levels only stress intensification around inclusions can explain the formation of cyclic–plastic strains (PSBs). They may lead to debonding of the interface or cracking of the inclusion itself. In the next section the debonding mechanism is described in detail for soft martensitic steel. The inclusion cracking results from multiple slip bands impinging upon the inclusion. The fatigue crack initiation may be explained by the criterion that a critical value of the accumulated self-strain energy is reached owing to dislocation dipole accumulation [7]. The micromechanism responsible for crack nucleation in the bulk should be the same as above, e.g. facilitated crack formation at PSBs in corrosion environments. An "inverted" mechanism, in which crack nucleation at PSBs in the bulk surrounding the inclusion leads first to crack nucleation

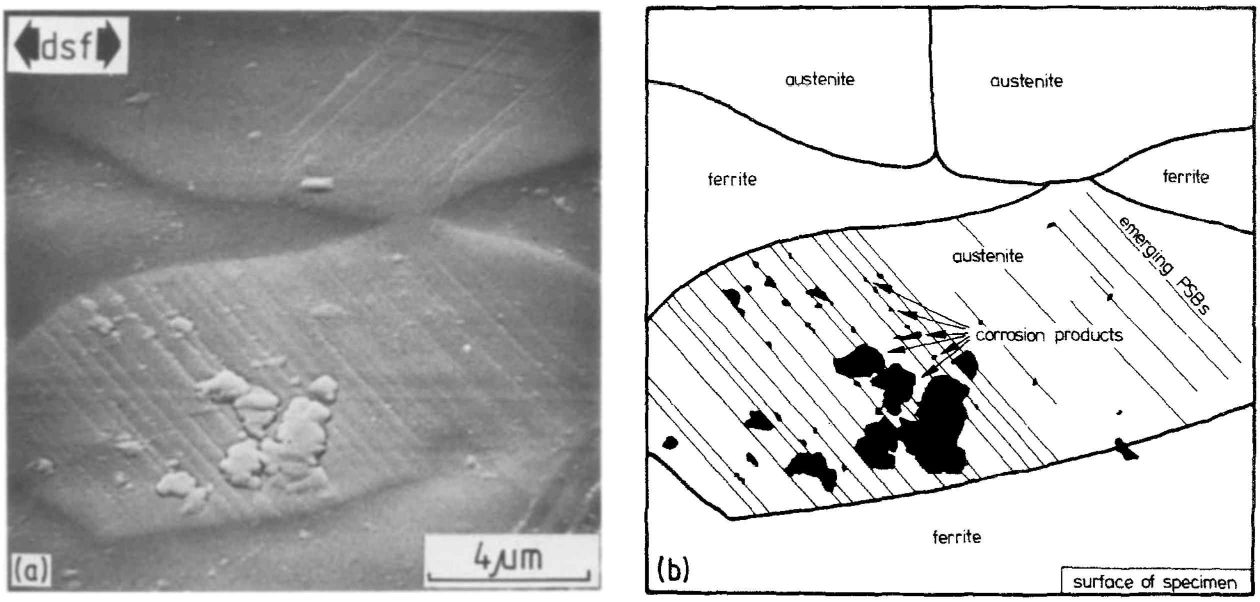

Figure 5 (a, b) Duplex steel: localized corrosion attack caused by emerging PSBs.

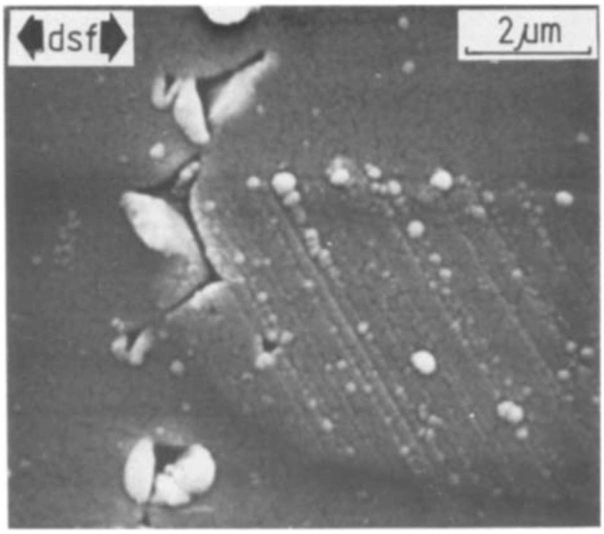

Figure 6 Duplex steel: crack initiation at PSBs in austenite or near phase boundaries at high stress levels (surface photograph).

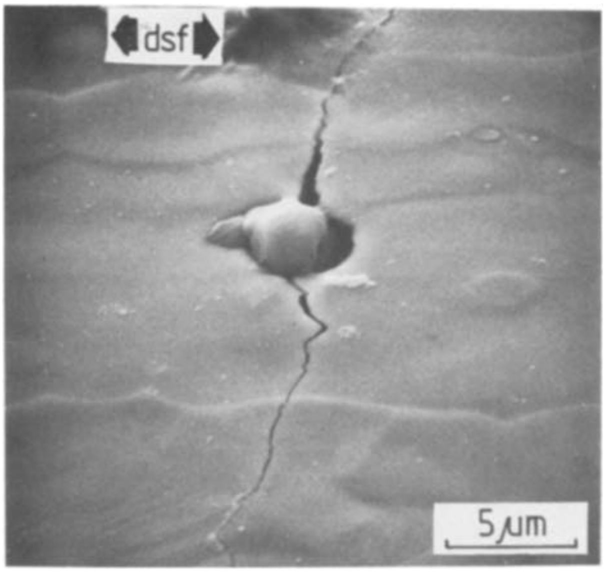

Figure 8 Duplex steel: crack initiation originating from a debonded inclusion (surface photograph).

and then to debonding or particle cracking, is also conceivable but is not very probable. For a perfectly bonded, rigid inclusion the theoretical maximum shear stress in a uniaxial stress field occurs at the tensile pole. Thus, crack nucleation due to activation of slip bands should be initiated at the tensile pole, a mechanism which has not been observed experimentally.

Corrosion fatigue crack initiation under stable passive corrosion conditions should not be possible if the applied loads do not lead to cyclic–plastic strain. Thus, there should be a corrosion fatigue limit similar to the fatigue limit measured in air. Certainly, this critical value may be lowered from the critical air value since an active environment affects near-surface phenomena and may thus also facilitate PSB formation.

3.3. Soft martensitic steel

These 16 % Cr–5 % Ni stainless steels show excellent technological properties and reasonable corrosion resistance. When polarization curves were measured, an increased tendency to pitting was detected at elevated (4.4 N NaCl) chloride concentrations at 80° C [15, 22].

The influence of the neutral solution temperature on the corrosion fatigue strength is much more significant than for the duplex steel, but less significant than for the 13 % Cr steel (Fig. 9). This is in keeping with the different stabilities of the passive film for these stainless steels. Macroscopically, a strong large-area

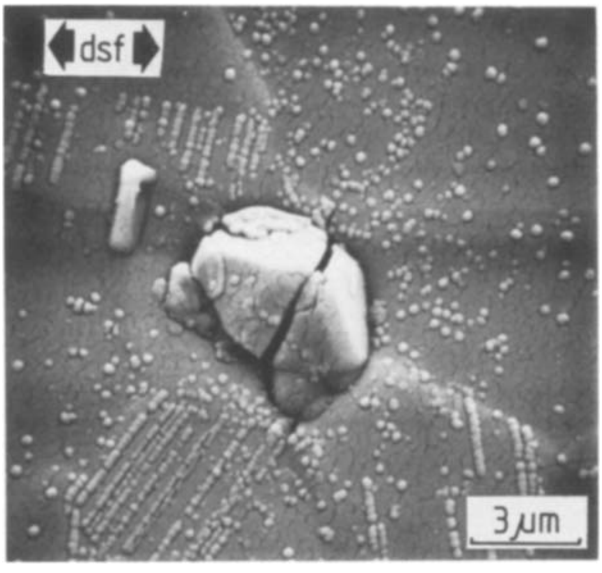

Figure 7 Duplex steel: crack initiation originating from a cracked inclusion (surface photograph).

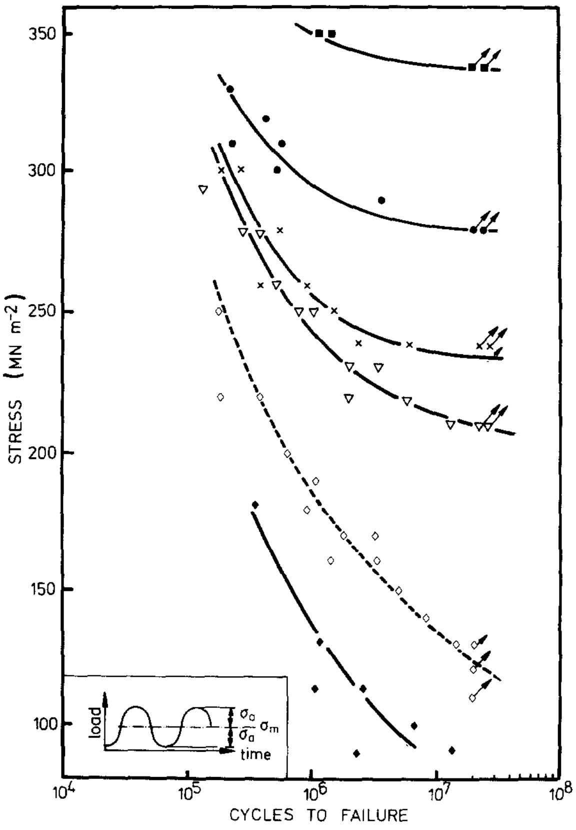

Figure 9 Soft martensitic steel: air and corrosion fatigue behaviour. (■) Air; (●) 20° C, 0.01 N NaCl; (x) 80° C, 0.01 N NaCl, (▽) 80° C, 4.4 N NaCl; (◆, ◇) 150° C, 0.01 N NaCl. All at σ_m = 350 MN m^{-2}, 50 Hz except (◇) which was at 250 MN m^{-2}.

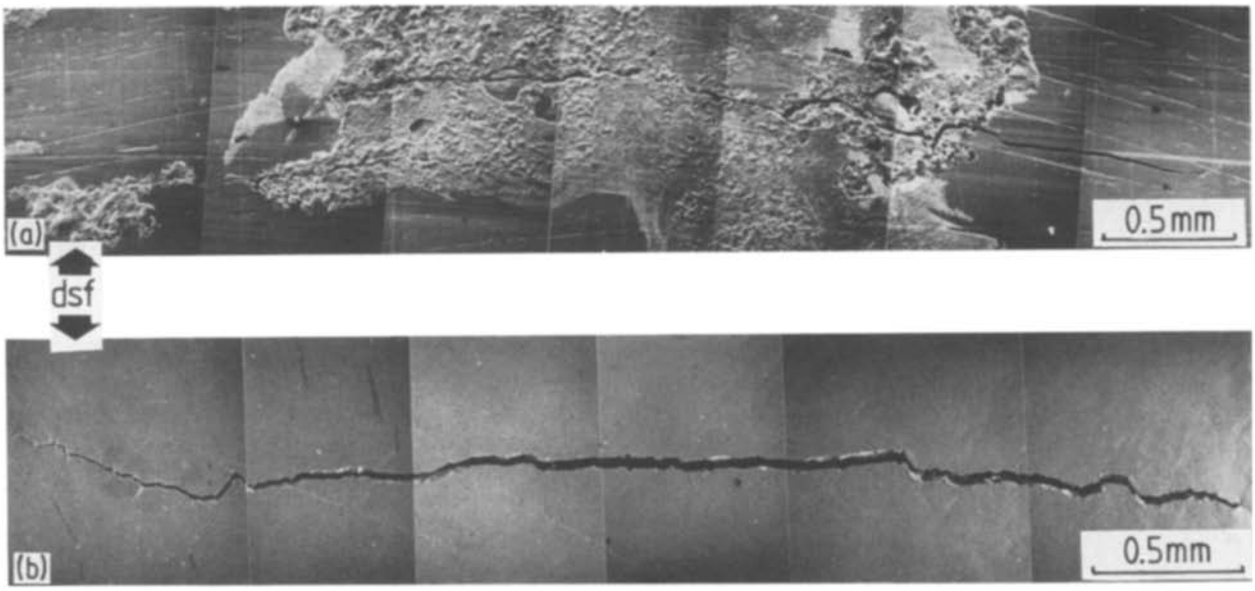

Figure 10 Soft martensitic steel: macroscopic features at specimen surface after crack propagation as a function of the stability of the passive film. (a) Pitting superposed, (b) stable passive.

corrosion attack can be detected at specimen surfaces after testing in 150° C solutions, whereas as with duplex steels, no corrosion features are (macroscopically) visible after testing in solutions with decreased temperature (Fig. 10). In this range the stability of the passive film is also maintained under additional dynamic loads.

In the stably passive range of corrosion behaviour, corrosion fatigue cracks in these martensitic steels are found to occur exclusively at inclusions (Fig. 11). An inclusion–matrix debonding mechanism seems to be the essential preliminary to the nucleation of a crack. A corrosion attack at the interface may facilitate or even induce this debonding. The inclusions found were mainly oxides. Sulphide-type inclusions, which are known to initiate corrosion fatigue cracks by corrosion of a sulphur-enriched band in the matrix around the inclusion [23], could not be detected in the fractured surfaces near the crack origin. Metallurgical inhomogeneities, such as prior austenite grain boundaries, will not affect the early stage of corrosion fatigue crack growth (Fig. 12).

The mechanism of corrosion fatigue crack initiation for these martensitic steels is very similar to that observed for the duplex steel. If the alloy exhibits stable passivity, crack nucleation always occurs at inclusions. The poor adhesion between the matrix and oxide inclusion, which is perhaps additionally lowered by corrosion, leads to debonding. Debonding of such a hard oxide inclusion in a soft matrix starts at the tensile pole of the inclusion and is followed by growth of the debonded seam in the direction of the equator of the inclusion. Finally, as a result of this mechanism an inclusion pit was formed which simply serves as stress raiser. The nucleation of the matrix crack itself is once more closely connected with PSB formation. For ordinary fatigue cracks Kunio *et al.* [5] pointed out that the same nucleation mechanism in martensitic steels and ductile materials is valid. The validity is also maintained in corrosive environments. Under

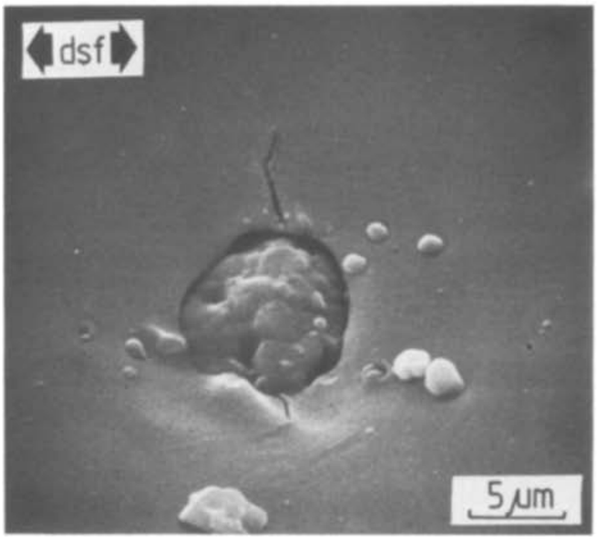

Figure 11 Soft martensitic steel: crack initiation originating from a debonded inclusion (surface photograph).

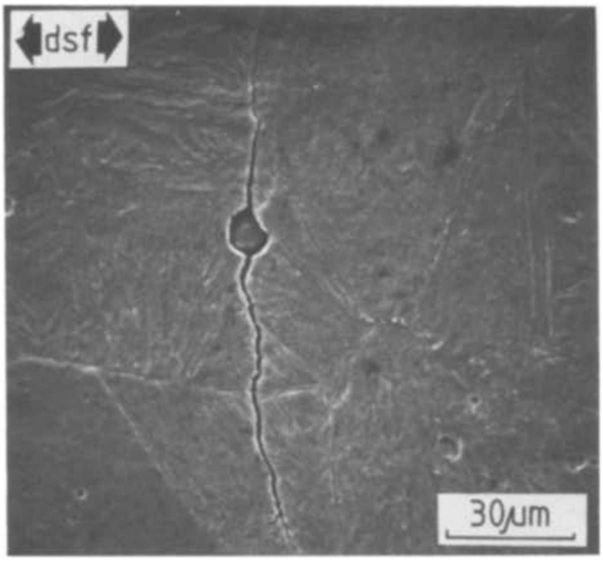

Figure 12 Soft martensitic steel: crack propagation on specimen surface (etched).

these stable passive corrosion conditions a corrosion fatigue limit still exists; it cannot be lower than the cyclic yield strength of the material regarding the lowering of this value by the corrosive environment.

At certain elevated temperatures the stability of the passive film is disturbed, and pitting will occur under these conditions. Here, the process of corrosion fatigue crack formation is comparable to the damage mechanism described for the 13% Cr steel. Indeed, the large-area corrosion attack on the specimen surface mainly occurs during crack propagation, and the corrosion pits themselves are less significant. Fractographic investigations show no indication of hydrogen-assisted crack initiation. As with the other two steels, the specimens will be damaged by only one or very few crack nucleations under conditions of stable passivity, but normally by more than one propagating corrosion fatigue crack under conditions of unstable passivity. In air, fatigue crack initiation is always associated with debonding of non-metallic particles.

A second alloy composition of this soft martensitic steel containing 2% Mo was also investigated. This variant shows a lower corrosion fatigue strength, which is mainly due to the different sizes and shapes of inclusion. The microfractographic features of the two alloys as a function of the chloride ion concentration and solution temperature are the same [14].

4. Conclusions

High-cycle corrosion fatigue tests with three different stainless steels in neutral NaCl solutions were carried out to investigate the mechanisms of initiation and early growth of cracks as well as their influence on the cyclic lifetime. The decrease in the fatigue limit from the value measured in air to that measured in corrosive environments is directly related to the stability of the protective passive film. One has to distinguish between active, unstably passive and stably passive corrosion fatigue behaviour; the last two were found to occur in these stainless steels.

If the material exhibits stable passivity in corrosive environments, the main results are as follows:

1. There is still a corrosion fatigue limit at a certain load level where the cyclic stresses cause no microplastic strains. Similar results was found by Mueller [24].
2. The stability of the passive film is also maintained under cyclic loads, and activated areas will be repassivated.
3. Crack nucleation is always associated with localized corrosion attack caused by emerging PSBs. Significant PSBs could only be found in (ductile) austenite grains. The facilitated and accelerated crack nucleation under corrosion fatigue conditions can be described as synergistic interaction between corrosion and fatigue.
4. In real high-cycle fatigue, stress intensifications around non-metallic inclusions lead to cyclic microplastic strains. These lead to debonding (possibly accelerated by corrosion attack) or inclusion cracking.
5. Only rigid oxide inclusions were found to affect the corrosion fatigue behaviour of these three stainless steels.
6. Crack nucleation in the bulk surrounding the cracked or debonded inclusion results from PSB activation.
7. Only one propagating crack can usually be detected.

If the stability of the passive film of the steels is (locally) disturbed, the important results are as follows:

1. There is no corrosion fatigue limit below which failure does not occur.
2. Besides the material properties, mainly the pit growth rate affects the corrosion fatigue behaviour. Enhanced dissolution at the base of the pit due to the cyclic loading may appear.
3. Under real high-cycle fatigue conditions, only stress intensifications at the base of the pit can explain the crack initiation.
4. In most cases few propagating cracks can be detected.
5. The mechanism of crack initiation can be described as a superposition of corrosion fatigue and pitting.

Acknowledgements

Most of this work is part of the PhD thesis of R. Mathis, carried out at the Institut für Werkstoffwissenschaften, Lehrstuhl für Metallurgie und Metallkunde, Technical University of Munich (FRG). The author wishes to thank Professor Schmitt-Thomas for supporting the investigations. Thanks are also due to Dr Sessler for permission to publish some of the test data in Section 3.1.

References

1. C. LAIRD, in: Fatigue and Microstructure, American Society for Metals, Materials Science Seminar, St. Louis, Missouri, 1978 (American Society for Metals, Ohio, 1979) p. 149.
2. W. A. WOOD, S. McK. CAUSLAND and K. R. SARGANT, *Acta Metall.* **11** (1963) 643.
3. L. M. BROWN, *Scripta Metall.* **11** (1977) 127.
4. P. NEUMANN, *Acta Metall.* **17** (1969) 1219.
5. T. KUNIO, M. SHIMIZU, K. YAMADA, A. SAKURA and T. YAMAMOTU, *Int. J. Fract.* **17** (1981) 111.
6. J. LANKFORD and F. N. KUSENBERGER, *Met. Trans.* **4** (1973) 553.
7. K. TANAKA and T. MURA, *ibid.* **13A** (1982) 293.
8. N. M. A. EID and P. F. THOMASON, *Acta Metall.* **27** (1979) 1239.
9. J. H. PAYER and R. W. STAEHLE, in Proceedings of NACE Conference Series Vol. 2; Corrosion Fatigue: Chemistry, Mechanics and Microstructure, Storrs, June 1971, Edited by A. J. McEvily and R. W. Staehle (National Association of Corrosion Engineers, Houston, Texas, 1972) p. 211.
10. R. M. PELLOUX, R. E. STOLTZ and J. A. MOSKOVITZ, *Mater. Sci. Eng.* **25** (1976) 193.
11. D. J. DUQUETTE, in Proceedings of NACE Conference Series Vol. 2; Corrosion Fatigue: Chemistry, Mechanics and Microstructure, Storrs, June 1971, Edited by A. J. McEvily and R. W. Steahle (National Association of Corrosion Engineers, Houston, Texas, 1972) p. 12.
12. T. C. LINDLEY, P. McINTYRE and P. J. TRANT, *Met. Tech.* **9** (1982) 135.
13. H. SPÄHN, *Z. Metalloberfläche* **16** (1962) 299.
14. C. PATEL, T. PYLE and V. ROLLINS, *Met. Sci.* **11** (1977) 185.
15. R. MATHIS, PhD thesis, Technical University of Munich (1983).

16. W. SESSLER, PhD thesis, Technical University of Munich (1984).
17. Z. SZKLARSKA-SMIALOWSKA, *Corrosion (National Association of Corrosion Engineers)* **28** (1972) 388.
18. R. N. PARKINS, *Met. Tech.* **9** (1982) 122.
19. D. HARDIE, *ibid.* **9** (1982) 143.
20. Kh. G. SCHMITT-THOMAS, H. MEISEL and R. MATHIS, *Arch. Eisenhüttenwesen* **53** (1982) 321.
21. J. A. MOSKOVITZ and R. M. PELLOUX, in Proceedings of the ASTM Conference on Corrosion-Fatigue Technology, Denver, November 1976, (American Society for Testing and Materials, Philadelphia, Pennsylvania, Special Technical Publication No. 642, 1978) p. 133.
22. Kh. G. SCHMITT-THOMAS, R. MATHIS and H. MEISEL, *Arch. Eisenhüttenwesen* **54** (1983) 412.
23. G. P. RAY, R. A. JARMAN and J. G. N. THOMAS, *Corros. Sci.* **25** (1985) 171.
24. M. P. MUELLER, *Corrosion (National Association of Corrosion Engineers)* **38** (1982) 431.

Received 15 April
and accepted 30 June 1986